

A Comparison of Acoustic Radiation Force-Derived Indices of Cardiac Function in the Langendorff Perfused Rabbit Heart

Maryam Vejdani-Jahromi, Mathew Nagle, Yang Jiang, Gregg E. Trahey, *Member, IEEE*,
and Patrick D. Wolf, *Member, IEEE*

Abstract—In the past decade, there has been an increased interest in characterizing cardiac tissue mechanics utilizing newly developed ultrasound-based elastography techniques. These methods excite the tissue mechanically and track the response. Two frequently used methods, acoustic radiation force impulse (ARFI) and shear-wave elasticity imaging (SWEI), have been considered qualitative and quantitative techniques providing relative and absolute measures of tissue stiffness, respectively. Depending on imaging conditions, it is desirable to identify indices of cardiac function that could be measured by ARFI and SWEI and to characterize the relationship between the measures. In this study, we have compared two indices (i.e., relaxation time constant used for diastolic dysfunction assessment and systolic/diastolic stiffness ratio) measured nearly simultaneously by M-mode ARFI and SWEI techniques. We additionally correlated ARFI-measured inverse displacements with SWEI-measured values of the shear modulus of stiffness. For the eight animals studied, the average relaxation time constant (τ) measured by ARFI and SWEI were (69 ± 18 ms, $R^2 = 0.96$) and (65 ± 19 ms, $R^2 = 0.99$), respectively (ARFI-SWEI inter-rater agreement = 0.90). Average systolic/diastolic stiffness ratios for ARFI and SWEI measurements were 6.01 ± 1.37 and 7.12 ± 3.24 , respectively (agreement = 0.70). Shear modulus of stiffness (SWEI) was linearly related to inverse displacement values (ARFI) with a 95% CI for the slope of 0.010 – 0.011 ($1/\mu\text{m}$)/(kPa) ($R^2 = 0.73$). In conclusion, the relaxation time constant and the systolic/diastolic stiffness ratio were calculated with good agreement between the ARFI- and SWEI-derived measurements. ARFI relative and SWEI absolute stiffness measurements were linearly related with varying slopes based on imaging conditions and subject tissue properties.

Index Terms—Acoustic radiation force impulse (ARFI) imaging, cardiac function, elastography, shear wave imaging.

I. INTRODUCTION

CARDIOVASCULAR disorders are one of the most prevalent causes of death worldwide. A significant number of patients suffer from heart failure with a decrease in their systolic and/or diastolic cardiac function. In systolic heart failure, the heart cannot contract effectively to eject the blood; in diastolic heart failure [also known as heart failure with preserved ejection fraction (HFpEF)], the heart cannot

fully relax to receive a sufficient amount of blood during diastole. For decades, researchers have been working to develop methods of quantifying cardiac function using measures of the dynamic material properties of the heart. These methods range from fully invasive techniques such as pressure-volume loop measurements (e.g., end diastolic pressure volume relationship (EDPVR) or end systolic pressure volume relationship (ESPVR) measurements) to the noninvasive ultrasound-based strain or Doppler imaging of the heart (e.g., E/A index). However, these techniques derive indirect measures of the material properties of the myocardium and are frequently dependent on load.

Recently, researchers have developed elasticity imaging techniques to directly assess the mechanical properties of tissue [1]–[4]. These techniques involve exciting the tissue and tracking the elastic response. Typically, acoustic radiation force is used to push the tissue. The force density generated by acoustic radiation can be calculated as

$$F = \frac{2\alpha I}{C} \quad (1)$$

where α equals the absorption coefficient of the medium, I equals the intensity of the ultrasound, and C equals the speed of sound through the medium. As the acoustic wave pushes the tissue, it generates a mechanical wave propagating perpendicular to the direction of the push. The velocity of this wave can be related to shear modulus and Young's modulus of stiffness using the formula

$$C_t = \sqrt{\frac{\mu}{\rho}} = \sqrt{\frac{E}{2(1+\nu)\rho}} \quad (2)$$

where C_t is the shear-wave velocity of propagation, μ is shear modulus, E is Young's modulus, ν is Poisson's ratio, and ρ the density of the tissue. When the magnitude of the on-axis displacement is used, for mechanical assessment of the tissue, the method is called acoustic radiation force impulse (ARFI) imaging. This displacement magnitude is related to the amount of force and the stiffness of the medium. Young's modulus of stiffness can be calculated, assuming a linearly elastic isotropic medium, using the formula

$$\sigma = E * \varepsilon \quad (3)$$

where σ is the stress, E is the Young's modulus, and ε is the strain. Although the displacement magnitude is measured and can be considered an estimate of ε , the force applied at

Manuscript received January 10, 2016; accepted March 12, 2016. Date of publication March 17, 2016; date of current version September 12, 2016. This work was supported by the National Institutes of Health (NIH) under Grant R01EB012484 and Grant R37HL096023.

The authors are with the Department of Biomedical Engineering, Duke University, Durham, NC 27708 USA (e-mail: maryam.vejdanijahromi@duke.edu)

Digital Object Identifier 10.1109/TUFFC.2016.2543026

the push location cannot be accurately determined because the intensity and attenuation coefficients are not known accurately. Therefore, the stiffness modulus of the medium (E) cannot be measured quantitatively using ARFI Imaging. However, these on axis displacements can be used to visualize the relative stiffness difference in the tissue along planes of constant intensity. This technique has been used in the laboratory and clinically to visualize liver tumors, breast lesions, and cardiac ablation lesions [1], [5], [6].

In order to quantify the stiffness of the tissue, the velocity of the generated shear wave can be converted to shear or Young's modulus of stiffness using (2) and assuming a linear, isotropic elastic medium. This technique is called shear-wave elasticity imaging (SWEI or SWI) [4]. This quantification of stiffness has proven useful in liver fibrosis characterization [1]. Therefore, ARFI and SWEI are considered qualitative and quantitative elastography techniques, respectively. When ARFI and SWEI measurements are recorded at one location through the cardiac cycle, the technique can be considered as an M-mode technique: M-mode ARFI and M-mode SWEI. In this paper, the terms ARFI and SWEI refer to M-mode versions of those measurements.

Recently, using ARFI and SWEI, we demonstrated the effect of coronary perfusion pressure on cardiac stiffness. The effects are known as the "garden hose" and "Gregg" effects for diastole and systole, respectively [7], [8]. In addition to investigating the factors affecting ARFI and SWEI, it is important to study potential functional indices of the heart that could be measured using ARFI and SWEI. One of the known functional indices of the heart is the relaxation time constant. The isovolumic relaxation time constant (τ) is used to characterize the active phase of cardiac relaxation using the exponential intraventricular pressure decline during early diastole. This value is measured clinically using indirect methods that correlate with the pressure-derived relaxation time constant [9]. This index has been shown to be inversely related to diastolic cardiac function and represents the active energy consumption portion of ventricular relaxation [10]. It has been shown that this index is useful in the diagnosis or therapeutic follow-up of patients with diastolic heart failure or HFpEF [9], [11]. The systolic/diastolic stiffness ratio is another potential functional index that provides a ratio-metric measure of the contractile and compliance states of the myocardium. This measure could be helpful in both systolic and diastolic heart failure diagnosis.

Although there are a few publications that have investigated SWEI measurements of cardiac function (e.g., [12]–[14]), to the best of our knowledge, there is no published research that has described relaxation time constant measurements of the heart using ARFI and SWEI. In this paper, we investigate the relationship between ARFI and SWEI measures of the relaxation time constant and the systolic/diastolic stiffness ratio.

II. MATERIALS AND METHODS

Eight white New Zealand rabbits (3.93 ± 0.28 kg) were studied in this protocol. The study was approved by the Institutional Animal Care and Use Committee (IACUC) at Duke University, and it conformed to the Guide for the Care and Use of

Laboratory Animals. A Langendorff preparation was used in these experiments. Rabbits were heparinized and anesthetized by Xylazine and Ketamine IM and IV until the reflexes disappeared. A bilateral thoracotomy was performed and the heart isolated and placed in Tyrode's solution at 0°C – 4°C . Tyrode's solution was made fresh on the day of the experiment and was used to perfuse coronary arteries retrogradely to keep the heart beating throughout the experiment. Unneeded tissue was excised, and a vent was placed in the left ventricle. The hearts were submerged in a saline bath, and an imaging probe was placed 10–15 mm from the epicardial surface of the heart in a short-axis view of the left ventricular free wall. The perfusion solution and the bath were kept at 37°C – 38°C . Additional details about the procedure and the experimental setup can be found in our previous publication [8].

A Sonoline Antares ultrasound scanner (Siemens Healthcare, Ultrasound Business Unit, Mountain View, CA, USA) was used for ARFI and SWEI Imaging. A linear VF10-5 probe was used with a push frequency of 5.7 MHz and a tracking frequency of 8 MHz. The push and tracking F-numbers were set to 1.5 and 2, respectively. The pulse repetition frequency used for the sequence was 4.3 kHz. A 300-cycle pulse was used to generate the ARF impulse. A sequence was developed to acquire 40 paired measurements of alternating ARFI and SWEI at a 35-Hz sampling frequency (1.2 s). The transmit focus was 16 mm. A scanner "fire" signal was recorded simultaneously with the electrocardiogram (ECG) signal using Powerlab/Labchart data acquisition system (ADInstruments, Colorado Springs, CO, USA) to allow synchronization of the scanner acquisitions and the cardiac cycle.

Tissue displacement was estimated using the Loupas algorithm [15]. The motion of the heart was subtracted from the displacement curves using a quadratic motion filter [16]. An example of displacement estimation before and after quadratic motion filtering is Fig. 1 of the referenced paper. For SWEI velocity estimations, the Radon Sum algorithm described by Rouze *et al.* was used [17]. Displacements were tracked on axis for ARFI and from 0 to 5 mm laterally for SWEI during the 5 ms following the push. The kernel length was 1.5 wavelengths. Data processing was done by a custom MATLAB program (The MathWorks, Natick, MA, USA).

Fig. 1 shows ARFI and SWEI and ECG measurements through the cardiac cycle in one of the isolated hearts. The calculated average inverse displacement is also shown. For all hearts, the ARFI displacements were averaged over the myocardial thickness. The mean and standard deviation of the displacements through myocardial depth for the subject in Fig. 1 was found to be 12 and 6 μm , respectively, over 228 pixels (3.9 mm) in the axial dimension. SWEI measurements of shear velocity were also calculated over the full thickness of the myocardium. The slope of shear-wave propagation was calculated using the above-mentioned methods. For the same diastolic timing of the Fig. 1 example, the standard deviation of the residuals for the time of maximal displacement points to the calculated slope of shear velocity was found to be 0.07 ms. For ARFI recordings, the displacement at 0.24 ms following the push was used as the measured value. Displacement values were converted to inverse displacement, as this is a surrogate of stiffness [18].

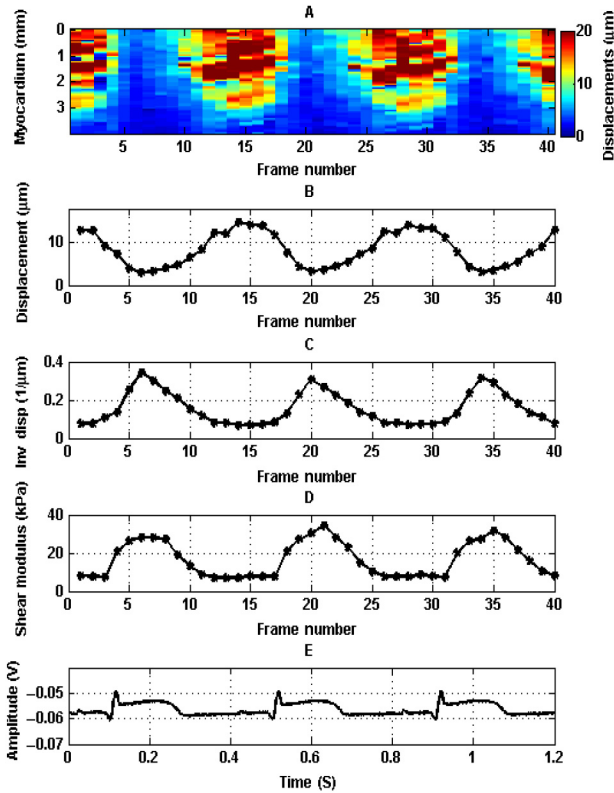


Fig. 1. Panel A shows the ARFI displacements in the left ventricular free wall during the cardiac cycle in one of the subjects. Panel B is the average displacements and panel C is the inverse of the average displacements through the cardiac cycle (a measure of stiffness). Panel D displays the shear modulus measurements from SWEI Imaging through the cardiac cycle and panel E presents the simultaneous ECG signal. It is clear that in systole and diastole, the stiffness of the left ventricular free wall increases and decreases, respectively, as shown by both the ARFI and SWEI measurements.

For each subject, a total of six acquisitions of 40 measurements were recorded through the cardiac cycle at the same location within 4 min. If the estimated displacements were negative or if the calculated SWEI slope yielded infinity, a linearly interpolated value was used for that point. This happened in 13 points of 1920 points recorded. In one instance, an extreme displacement estimation was replaced by a two-point linearly interpolated value. These noisy data points are usually due to speckle decorrelation caused by out of plane motion of the heart. Changes in speckle patterns for the displacement estimation would result in displacement measurement error. Panel A in Fig. 2 shows the ARFI inverse displacement through the cardiac cycle, and panel C shows the shear modulus of stiffness calculated by squaring the shear velocity through the cardiac cycle. The relaxation time constant (τ) is typically measured by an exponential curve fit of the intraventricular pressure during diastolic isovolumic relaxation [19], [20]. The start of this relaxation period corresponds to the time of aortic valve closure. This point is usually identified using the minimum intraventricular dp/dt . The following equation shows the expected relationship, where p , t , and τ are the intraventricular pressure, time, and relaxation time constant, respectively:

$$p = p_0 e^{-\frac{t}{\tau}}. \quad (4)$$

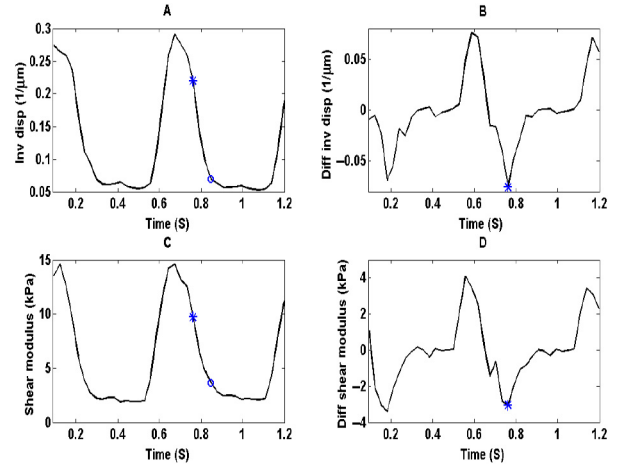


Fig. 2. Example of relaxation time constant measurement in one of the subjects. Panels A and C show the inverse displacement and shear modulus measurement of stiffness recorded by ARFI and SWEI imaging, respectively. Panels B and D display the derivative of the curves in panels A and C. The location of the minimum ($d_{\text{stiffness}}/dt$) was used as the starting point of isovolumic relaxation (blue asterisk). The end point (blue circle) was set to 87 ms (3 time points) after the starting point.

Panels B and D in Fig. 2 show the derivative of the inverse displacement and shear modulus curves measured through the cardiac cycle. The local minimum time derivative of the ARFI or SWEI signal close to the mid isovolumic relaxation of the cardiac cycle was found and used as the starting point. The end point for the relaxation period usually considers the time when the intraventricular pressure is 5 mmHg above the end diastolic pressure. Since the sampling rate was not high enough corresponding to the changes of stiffness in this period of the cardiac cycle, a fixed duration was used for the end point of relaxation curve. This was set to be 3 samples after the starting point, equal to 87 ms. These 4 points were fit to an exponential curve, and τ was calculated for ARFI and for SWEI measurements. Although it would be desirable to have more samples during this time to obtain a more accurate curve fit, this was the highest sampling rate at which the scanner could record ARFI/SWEI data.

The systolic/diastolic stiffness ratio was calculated using both ARFI and SWEI measurements

$$\frac{\text{Systolic_Stiffness}}{\text{Diastolic_Stiffness}}. \quad (5)$$

For each subject, a total of six measurements of the ratio were calculated. The P-wave of the ECG was used to identify the diastolic frame in the ARFI and SWEI measurements. Because it is challenging to find the time of maximum systolic stiffness from the ECG, we used the point with the maximum inverse displacement of the ARFI and SWEI stiffness measurements over the entire cardiac cycle as the measurement point.

Statistical analysis was done using R and MATLAB programs. To measure the agreement between ARFI and SWEI measurements of the relaxation time constant and the systolic/diastolic ratio, intraclass correlation analysis was performed to assess the inter-rater reliability [21]. To establish a

TABLE I
RELAXATION TIME CONSTANT (τ) MEASUREMENTS IN (MS) USING ARFI AND SWEI (SHEAR MODULUS) MEASUREMENTS OF STIFFNESS

Subjects	1	2	3	4	5	6	7	8	Average
ARFI (τ)	64.17	105.47	51.54	53.68	73.55	78.29	51.70	76.46	69.36
ARFI (τ), standard deviation	16.60	9.93	6.56	2.84	11.31	8.12	5.12	28.46	11.12
ARFI (τ), R^2	0.96	0.99	0.92	1.00	0.98	0.99	0.94	0.91	0.96
SWEI (τ)	51.17	86.75	42.94	58.65	90.16	76.84	43.39	68.66	64.82
SWEI (τ), standard deviation	3.24	9.61	4.08	3.33	4.50	5.77	2.43	2.07	4.38
SWEI (τ), R^2	0.98	0.99	0.99	0.99	0.99	1.00	0.99	0.99	0.99

TABLE II
SYSTOLIC/DIASTOLIC RATIO OF MYOCARDIAL STIFFNESS MEASUREMENTS USING ARFI AND SWEI (SHEAR MODULUS) MEASUREMENTS OF STIFFNESS

Subjects	1	2	3	4	5	6	7	8	Average
ARFI ratio	5.99	4.09	6.75	6.94	5.27	4.62	8.35	6.08	6.01
ARFI ratio, standard deviation	0.39	0.36	0.40	0.26	0.61	0.40	1.02	0.45	0.49
SWEI ratio	8.45	3.96	8.28	6.25	4.21	6.98	13.91	4.91	7.12
SWEI ratio, standard deviation	0.66	0.37	0.67	0.84	0.60	0.83	1.06	0.73	0.72

model for all rabbits, a multivariable linear regression model was used treating the subject as an independent variable.

III. RESULTS

Table I shows a summary of the relaxation time constant (τ) data measured based on ARFI inverse displacement curves. The average (τ) was 69 ± 18 ms ($R^2 = 0.96$). The mean of the shear modulus-derived measures of relaxation time was 65 ± 19 ms ($R^2 = 0.99$). The table also lists standard deviations of intrasubject measurements ($n = 6$). The average standard deviations of the intrasubject measurements were 11 and 4 ms for ARFI- and SWEI-determined measures, respectively. This within subject variation is less than the between subject variability of 18 and 19 ms. The intraclass correlation for inter-rater agreement of ARFI and SWEI measurements was calculated to be 0.90 indicating strong agreement between the measurements.

The systolic/diastolic stiffness ratios based on ARFI and SWEI recording are listed for all the subjects in Table II. The average ratio for ARFI and shear modulus recordings was 6.01 ± 1.37 and 7.12 ± 3.24 , respectively. The agreement between ARFI and SWEI for systolic/diastolic ratio measurements, assessed by inter-rater reliability test, was 0.70. In addition, Table II reports the intrasubject repeatability of the

measurements. The average standard deviation of the intrasubject measurements, 0.49 and 0.72 ms for ARFI and SWEI, respectively, were much less than the between subject variability of 1.37 and 3.24 ms.

A linear regression model was used to compare the material stiffness values from ARFI and SWEI. Fig. 3 shows the shear modulus of stiffness through the cardiac cycle versus inverse displacement stiffness calculations from ARFI for 1.2 s of the cardiac cycle in each of the subjects. The slope of the regression line and the R^2 values are listed for each subject. Fig. 4 shows the results of the multivariate linear regression. Plotted are the measured values of inverse displacement as a function of the inverse displacement predicted from a shear modulus regression model that accounts for between subject differences in which each subject is treated as an independent variable with a different slope. The shear modulus of stiffness was linearly related to inverse displacement stiffness values from ARFI with a 95% confidence interval of 0.010–0.011 (1/ μ m)/(kPa) ($R^2 = 0.73$, residual standard error = 0.054).

IV. DISCUSSION

In this study, we have compared ARFI and SWEI measurements of the relaxation time constant (τ) and the systolic/diastolic ratio for cardiac functional assessment. ARFI

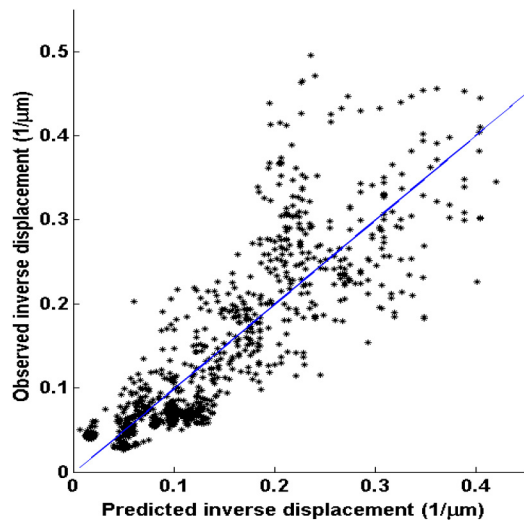


Fig. 3. Results of the multivariate linear regression. The measured values of inverse displacement are plotted as a function of the inverse displacement predicted from a shear modulus regression model that accounts for between subject differences. The shear modulus of stiffness was linearly related to inverse displacement stiffness values from ARFI.

and SWEI measurements of these functional indices were in agreement with each other, with the relaxation time constant having stronger agreement than systolic/diastolic ratio. This is to be expected because the time constant is a least-squares fit derived from four points while the ratio is the quotient of two points, all with the same level of noise. In addition, the relationship between ARFI and SWEI measurements of stiffness for myocardial tissue characterization was identified. We showed that inverse displacement relative stiffness measured by ARFI is linearly related to shear modulus measured by SWEI Imaging.

Although it is desirable to have SWEI-generated modulus of stiffness measurements throughout the cardiac cycle, imaging conditions and signal-to-noise ratio could make this challenging. The shear-wave amplitude at the lateral locations used to measure velocity must be large enough to be detectable. The displacement at these lateral locations is reduced by diffraction and absorption relative to the on-axis displacements used in ARFI imaging. For example in one of our subjects, the on-axis ARFI displacement during diastole was $12\ \mu\text{m}$, while the associated shear-wave amplitude of displacement dropped $3\ \mu\text{m}$ over $3\ \text{mm}$ of lateral propagation. Tracking shear-wave displacements becomes even more challenging, as the heart stiffens in systole. This increases the strength of push needed for a quality estimate [22]. It is important to note that with available scanners and the current FDA limits, transthoracic delivery of sufficient push strength could be challenging [23]. In addition, a meta-analysis review article, published in 2015, investigated ARFI and SWEI techniques for differentiating breast lesion malignancies reported that ARFI was less affected than SWEI by the inhomogeneity of breast lesions [6]. Considering the myocardium is also a heterogeneous medium (e.g., the vascular distribution pattern), further studies are needed to investigate if this is an important effect in the heart. Consequently, it is important to identify indices of cardiac function that could be measured by ARFI and to characterize their relationship to identical SWEI-derived measures.

Schiereck *et al.* studied the relaxation time constant in the rabbit Langendorff preparation. Using a custom pump, they were able to adjust the intraventricular volume and to record the left ventricular pressure (P). Relaxation time constant was calculated by linear approximation of the $\ln(P) - t$, where P is the intraventricular pressure over a 40-ms period starting 20 ms after the minimum of (dp/dt) . They found the relaxation time constant as a function of end diastolic volume (EDV) to be in the range of 34–63 ms [24], [25]. Our time constant measurements are at the upper end of their results corresponding to a 1.8-ml EDV. We would expect our results to correspond to their lower EDV measurements, and there could be several reasons for the difference. This could be due to a difference in the starting and ending points of the exponential curve fit, to aortic valve leakage causing a higher EDV in our preparation or could be due to differences in the calcium concentration of our perfusates.

Zile *et al.* reported that the relaxation time constant was $59 \pm 14\ \text{ms}$ in 47 diastolic heart failure patients compared to $35 \pm 10\ \text{ms}$ in 10 normal controls. This study was done using intraventricular pressure measurements [26]. Using MR elastography, Elgeti *et al.* and Tzschatzsch *et al.* measured the relaxation time constants in healthy human subjects which were 75 and 69 ms, respectively. In 11 patients with diastolic dysfunction, the relaxation time constant was found to be 134 ms, significantly longer than in healthy subjects. Although the MR elastography-based method of calculating the relaxation time constant was different from the method used in our study, these results demonstrate that elastography techniques can be used to measure the relaxation time constant for diastolic dysfunction assessment of the heart [27], [28].

Measurement of the relaxation time constant using ARF methods appears promising for diastolic heart failure assessment due to the low within subject variability compared to the increase seen in diastolic heart failure patients. Our within subject variability was less than 20% based on values reported in Table I, the time constant increase for patients in failure was more than 70% [26], [27]. Further studies are needed to investigate the exact relationship between the relaxation time constant measured by intraventricular pressure and ARFI or SWEI methods.

The systolic/diastolic ratio has been measured using several different methods. Using the stress and strain relationship, this ratio was estimated to be 4.2 in rats [29]. Using ARFI in canine hearts, Hsu *et al.* measured this value to be 5.3 [16]. Using SWEI elasticity measurements, the systolic-to-diastolic ratio was found to be 3.7 in ovine and canine hearts [30]. This ratio was measured to be 5.1 using shear-wave elastography in isolated rat hearts [13]. The shear modulus of stiffness ratio has been reported to be 6.3 and 14 in human hearts using MR elastography [31], [32]. Using ARFI and SWEI, our experiments found the ratio to be 6.0 and 7.1 in the isolated nonworking rabbit heart. These values are in a similar range as the values found in the literature, with the exception of one of the values derived from an MR elastography study. This could be due to the difference in the experimental procedure, species differences, or the difference in the assumptions used to calculate shear modulus.

Our results also show that shear modulus of stiffness is linearly related to inverse displacement measured by ARFI.

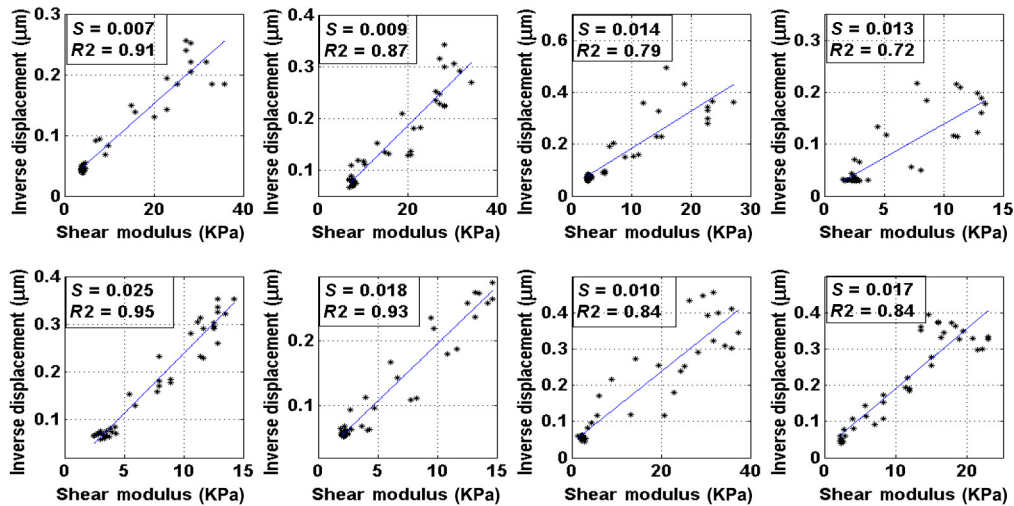


Fig. 4. Shear modulus of stiffness measured by SWEI imaging versus inverse displacement measurement of stiffness recorded by ARFI during 1.2 s of cardiac cycle in each subject. For each subject, the linear regression slope (S) and R^2 values are reported.

This is consistent with equation number (3). Inverse displacement was found to be linearly related to shear modulus of stiffness in phantom and in human prostate [18], [33]. Modeling the heart as an active phantom that constantly changes stiffness, our results indicate that this linear relationship holds through the cardiac cycle. We found a very high correlation result when we allowed the slope of the relationship to vary from subject to subject. In this experiment, a constant imaging plane was used for each subject. Between-subject variability of measurements could be caused by multiple factors including the intrinsic state of the myocardium and the fiber orientation in the specific imaging plane. However, from our results, it can be concluded that at a given spatial location in a specific heart, the linear relationship between ARFI and SWEI measurements holds throughout the cardiac cycle. The linear relationship between inverse displacement and shear modulus is likely the reason for the consistency between the ARFI- and SWEI-measured systolic/diastolic ratios and relaxation time constants.

We also calculated the relaxation time constant and the systolic/diastolic ratio using shear velocity data as opposed to shear modulus estimates. The relaxation time constants based on shear velocity were also calculated and found to be 136 ± 35 ms ($R^2 = 0.96$). Shear velocity time constants were on average 2 times larger than the shear modulus or ARFI-measured time constants consistent with what is expected from the relaxation time constant formula (4). The average of systolic/diastolic ratio measured using shear velocity was 2.61 ± 0.53 , which is the square of the shear modulus derived ratio. Shear velocity was linearly related to inverse displacement measurements with 95% confidence interval of 0.072–0.077 $(1/\mu\text{m})/(\text{m/s})$ ($R^2 = 0.78$, residual standard error = 0.049).

Grossman *et al.* have shown that $(dp/dt)_{\text{max}}/p$ is an index for cardiac contractility [34]. It has been shown that the stiffness measurements of myocardium through the cardiac cycle are linearly related to intraventricular pressure; therefore, similar parameters could be derived from stiffness curves throughout the cardiac cycle [13], [35]. In this study, we did not measure the $(d(\text{stiffness})/dt)_{\text{max}}/(\text{stiffness})$ as a measure of

contractility for two reasons. First, in this study, we used a Langendorff preparation with isolated hearts in which the heart is perfused retrograde through the aorta and the ventricle does not eject fluid as it contracts. Thus, there is little or no intraventricular pressure. This is also the reason we could not compare our elasticity-derived measures of the relaxation time constant with the more traditional pressure-derived measure. Second, we think that a higher sampling rate through the cardiac cycle is needed to accurately quantify $(d(\text{stiffness})/dt)_{\text{max}}/(\text{stiffness})$.

It has been shown that SWEI stiffness measurements are affected by fiber orientation [30], [36], [37]. It is possible that the focal configuration of the excitation pulse affects ARFI displacements in an anisotropic medium. This was shown by Hossain *et al.* using the finite-element method [38]. The effect of fiber orientation on ARFI measurements has not been fully investigated in cardiac tissue; it is expected that ARFI measurements are affected by them too due to the relationship between displacement and stiffness measurements. In these experiments, we did two things to mitigate the effects of fiber orientation. First, we imaged the same location consistently in each subject. Thus, within-subject variation due to fiber orientation should have been minimized. Second, we used displacement and SWEI measurements over the full thickness of the myocardium, resulting in a measurement at multiple fiber angles. Further studies are needed to characterize the effect of anisotropy on ARFI and SWEI measurements. In addition, our results are based on a linearly elastic model. If viscoelastic models are used to interpret SWEI measurements, it would be important to identify the relationship between both the elastic and viscous moduli and ARFI relative stiffness measurements [39]. As the shear wave propagates through a viscoelastic medium, its velocity will be affected by dispersion [40], [41]. We performed two-dimensional Fourier analysis of wave propagation at normal perfusion pressure in diastole. In all of the subjects, a prominent peak was observed with a mean frequency of (157 Hz). In six of the subjects, a smaller peak at higher frequency (average at 450 Hz) was also observed. Furthermore, Lamb waves and surface waves may be produced

in myocardium in addition to shear waves depending on the myocardial thickness, on the wave frequency, on the characteristics of the push, and on the location of measurements. Nenadic *et al.* investigated the relationship between the velocity of these types of waves and factors affecting them and showed that shear-wave velocity could be related to the velocity of Lamb-Rayleigh waves [42]. Therefore, variations in the shear velocity propagation might be affected by other parameters in addition to stiffness, and this needs further investigation.

V. CONCLUSION

In conclusion, ARFI and SWEI can be used to measure the cardiac functional indices of systolic/diastolic ratio and relaxation time constant. Although ARFI does not provide an absolute number for myocardial stiffness, it still can be used to assess cardiac function by measuring proportional or time dependent indices such as these. We showed that for constant imaging conditions, the inverse displacement measurement of stiffness provided by ARFI is linearly related to shear modulus of stiffness recorded by SWEI imaging and this is a key point for further investigation. Both ARFI and SWEI elastography techniques may be implemented on some ultrasound scanners and could provide a portable, cost efficient, noninvasive assessment of cardiac function.

ACKNOWLEDGMENT

The authors would like to thank E. Dixon-Tulloch and Duke Ultrasound Group for their help with this project. They also would like to thank Siemens Healthcare for their hardware system and technical support.

REFERENCES

- [1] J. R. Doherty, G. E. Trahey, K. R. Nightingale, and M. L. Palmeri, "Acoustic radiation force elasticity imaging in diagnostic ultrasound," *IEEE Trans. Ultrason., Ferroelectr., Freq. Control*, vol. 60, no. 4, pp. 685–701, Apr. 2013.
- [2] R. Sinkus, "Elasticity of the heart, problems and potentials," *Curr. Cardiovasc. Imag. Rep.*, vol. 7, no. 9, p. 9288, Aug. 2014.
- [3] K. R. Nightingale, M. L. Palmeri, R. W. Nightingale, and G. E. Trahey, "On the feasibility of remote palpation using acoustic radiation force," *J. Acoust. Soc. Amer.*, vol. 110, no. 1, pp. 625–634, 2001.
- [4] Ar. P. S. Sarvazyan, O. Rudenko, S. Swanson, B. Fowlkes, and S. Emelianov, "Shear wave elasticity imaging: A new ultrasonic technology of medical diagnostics," *Ultrasound Med. Biol.*, vol. 24, no. 9, pp. 1419–1435, 1998.
- [5] S. A. Eyerly, M. Vejdani-jahromi, D. M. Dumont, G. E. Trahey, and P. D. Wolf, "The evolution of tissue stiffness at radiofrequency ablation sites during lesion formation and in the Peri-Ablation period," *J. Cardiovasc. Electrophysiol.*, vol. 26, no. 9, pp. 1009–1018, 2015.
- [6] D. Li *et al.*, "Acoustic radiation force impulse elastography for differentiation of malignant and benign breast lesions: A meta-analysis," *Int. J. Clin. Exp. Med.*, vol. 8, no. 4, pp. 4753–4761, 2015.
- [7] M. Vejdani-jahromi, Y. Jiang, G. E. Trahey, and P. D. Wolf, "M-mode ARFI imaging demonstrates the effect of coronary perfusion on cardiac stiffness," in *Proc. IEEE Int. Ultrason. Symp.*, 2014, pp. 113–116.
- [8] M. Vejdani-jahromi, M. Nagle, G. E. Trahey, and P. D. Wolf, "Ultrasound shear wave elasticity imaging quantifies coronary perfusion pressure effect on cardiac compliance," *IEEE Trans. Med. Imag.*, vol. 34, no. 2, pp. 465–473, Feb. 2015.
- [9] E.-M. Jeong and S. C. Dudley, Jr., "Diastolic dysfunction," *Circ. J.*, vol. 79, no. 3, pp. 470–477, 2015.
- [10] E. Schertel, "Assessment of left-ventricular function," *Thorac Cardiovasc. Surg.*, vol. 2, pp. 248–254, 1998.
- [11] D. Gross, "Measuring cardiac function," in *Animal Models in Cardiovascular Research*. New York, NY, USA: Springer, 2009, pp. 65–91.
- [12] C. Pislaru, M. W. Urban, S. V. Pislaru, R. R. Kinnick, and J. F. Greenleaf, "Viscoelastic properties of normal and infarcted myocardium measured by a multifrequency shear wave method: Comparison with pressure-segment length method," *Ultrasound Med. Biol.*, vol. 40, no. 8, pp. 1785–1795, Aug. 2014.
- [13] M. Pernot, M. Couade, P. Mateo, B. Crozatier, R. Fischmeister, and M. Tanter, "Real-time assessment of myocardial contractility using shear wave imaging," *J. Amer. Coll. Cardiol.*, vol. 58, no. 1, pp. 65–72, Jun. 2011.
- [14] R. R. Bouchard, S. J. Hsu, P. D. Wolf, and G. E. Trahey, "In vivo cardiac, acoustic radiation force driven, shear wave velocimetry," *Ultrason. Imag.*, vol. 31, no. 4, pp. 201–213, 2009.
- [15] T. Loupas, J. T. Powers, and R. W. Gill, "An axial velocity estimator for ultrasound blood flow imaging, based on a full evaluation of the Doppler equation by means of a two-dimensional autocorrelation approach," *IEEE Trans. Ultrason., Ferroelectr., Freq. Control*, vol. 42, no. 4, pp. 672–688, Jul. 1995.
- [16] S. J. Hsu, R. R. Bouchard, D. M. Dumont, P. D. Wolf, and G. E. Trahey, "In vivo assessment of myocardial stiffness with acoustic radiation force impulse imaging," *Ultrasound Med. Biol.*, vol. 33, no. 11, pp. 1706–1719, Nov. 2007.
- [17] N. C. Rouze, M. H. Wang, M. L. Palmeri, and K. R. Nightingale, "Robust estimation of time-of-flight shear wave speed using a radon sum transformation," *IEEE Trans. Ultrason., Ferroelectr., Freq. Control*, vol. 57, no. 12, pp. 2662–2670, Dec. 2010.
- [18] S. Rosenzweig *et al.*, "Comparison of concurrently acquired in vivo 3D ARFI and SWEI images of the prostate," in *Proc. IEEE Int. Ultrasonics Symp. (IUS)*, 2012, pp. 97–100.
- [19] K. Yamamoto, "The time constant of left ventricular relaxation: Extrication from load dependence and overestimation of functional abnormality," *Circ. Heart Fail.*, vol. 3, no. 2, pp. 178–180, Mar. 2010.
- [20] D. A. Kass, "Assessment of diastolic dysfunction," *Cardiol. Clin.*, vol. 18, no. 3, pp. 571–586, 2000.
- [21] K. Gwet, *Handbook of Inter-Rater Reliability: The Definitive Guide to Measuring the Extent of Agreement Among Multiple Raters, Advanced Analytics, LLC*, 3rd edition, Mar. 2012, pp. 1–294.
- [22] D. P. Bradway, *Transthoracic Cardiac Acoustic Radiation Force Impulse Imaging*, Dissertation, Department of Biomedical Engineering, Duke University, 2013.
- [23] P. Song *et al.*, "Improved shear wave motion detection using pulse-inversion harmonic imaging with a phased array transducer," *IEEE Trans. Med. Imag.*, vol. 32, no. 12, pp. 2299–2310, Sep. 2013.
- [24] P. Schiereck, J. H. M. Nieuwenhuijs, E. L. de Beer, M. W. J. Van Hensen, F. A. M. Van Kaam, and A. Crowe, "Relaxation time constant of isolated rabbit left ventricle," *Amer. J. Physiol.*, vol. 253, no. 3, pp. 512–518, 1987.
- [25] P. J. M. Kil and P. Schiereck, "Influence of the velocity of changes in end-diastolic volume on the starling mechanism of isolated left ventricles," *Eur. J. Physiol.*, vol. 396, pp. 243–253, 1983.
- [26] M. R. Zile, C. F. Baicu, and W. H. Gaasch, "Diastolic heart failure—Abnormalities in active relaxation and passive stiffness of the left ventricle," *New Eng. J. Med.*, vol. 350, pp. 1953–1959, 2004.
- [27] T. Elgeti, M. Beling, B. Hamm, J. Braun, and I. Sack, "Elasticity-based determination of isovolumetric phases in the human heart," *J. Cardiovasc. Magn. Reson.*, vol. 12, no. 1, p. 60, Jan. 2010.
- [28] H. Tzschätzsch *et al.*, "Isovolumetric elasticity alteration in the human heart detected by in vivo time-harmonic elastography," *Ultrasound Med. Biol.*, vol. 39, no. 12, pp. 2272–2278, Sep. 2013.
- [29] J. E. Jalil, C. W. Doering, J. S. Janicki, R. Pick, S. G. Shroff, and K. T. Weber, "Fibrillar collagen and myocardial stiffness in the intact hypertrophied rat left ventricle," *Circ. Res.*, vol. 64, pp. 1041–1050, 1988.
- [30] R. R. Bouchard, P. D. Wolf, S. J. Hsu, D. M. Dumont, and G. E. Trahey, "Acoustic radiation force-induced shear wave propagation in cardiac tissue," *Ultrason. Imag. Signal Process.*, vol. 7265, pp. 726512–726518, Feb. 2009.
- [31] H. Tzschätzsch *et al.*, "In vivo time harmonic elastography of the human heart," *Ultrasound Med. Biol.*, vol. 38, no. 2, pp. 214–222, Feb. 2012.
- [32] I. Sack, J. Rump, T. Elgeti, A. Samani, and J. Braun, "MR elastography of the human heart: Noninvasive assessment of myocardial elasticity changes by shear wave amplitude variations," *Magn. Reson. Med.*, vol. 61, no. 3, pp. 668–677, Mar. 2009.
- [33] L. Zhai *et al.*, "Characterizing stiffness of human prostates using acoustic radiation force," *Ultrason. Imag.*, vol. 213, no. 32, pp. 201–213, 2010.

- [34] B. W. Grossman, H. Brooks, S. Meister, H. Sherman, and L. Dexter, "New technique for determining instantaneous myocardial force-velocity relations in the intact heart," *Circ. Res.*, vol. 28, pp. 290–298, 1971.
- [35] A. Kolipaka, K. P. McGee, A. Manduca, N. Anavekar, R. L. Ehman, and P. A. Araoz, "In vivo assessment of MR elastography-derived effective end-diastolic myocardial stiffness under different loading conditions," *J. Magn. Reson. Imag.*, vol. 33, no. 5, pp. 1224–1228, May 2011.
- [36] M. Couade *et al.*, "In vivo quantitative mapping of myocardial stiffening and transmural anisotropy during the cardiac cycle," *IEEE Trans. Med. Imag.*, vol. 30, no. 2, pp. 295–305, Feb. 2011.
- [37] W.-N. Lee *et al.*, "Mapping myocardial fiber orientation using echocardiography-based shear wave imaging," *IEEE Trans. Med. Imag.*, vol. 31, no. 3, pp. 554–562, Mar. 2012.
- [38] M. Hossain and C. M. Gallippi, "Estimation of degree of anisotropy in Transversely Isotropic (TI) elastic materials from Acoustic Radiation Force (ARF) -Induced peak displacements," in *Proc. IEEE Ultrason. Symp.*, 2015, pp. 1–4.
- [39] M. W. Urban, S. Chen, and M. Fatemi, "A review of Shearwave Dispersion Ultrasound Vibrometry (SDUV) and its applications," *Curr. Med. Imag. Rev.*, vol. 8, no. 1, pp. 27–36, 2012.
- [40] I. Z. Nenadic, M. W. Urban, S. A. Mitchell, and J. F. Greenleaf, "Lamb Wave Dispersion Ultrasound Vibrometry (LDUV) Method for quantifying mechanical properties of viscoelastic solids," *Phys. Med. Biol.*, vol. 56, no. 7, pp. 2245–2264, 2011.
- [41] C. Pislaru, M. W. Urban, I. Nenadic, and J. F. Greenleaf, "Shearwave dispersion ultrasound vibrometry applied to in vivo myocardium," in *Proc. IEEE Int. Conf. Eng. Med. Biol. Soc.*, Jan. 2009, vol. 2009, pp. 2891–2894.
- [42] I. Z. Nenadic, M. W. Urban, M. Bernal, and J. F. Greenleaf, "Phase velocities and attenuations of shear, Lamb, and Rayleigh waves in plate-like tissues submerged in a fluid (L)," *J. Acoust. Soc. Amer.*, vol. 130, no. 6, pp. 3549–3552, Dec. 2011.



Maryam Vejdani-Jahromi received the M.D. degree from Tehran University of Medical Sciences (TUMS), Tehran, Iran, in 2008. She is currently pursuing the Ph.D. degree in biomedical engineering at Duke University, Durham, NC, USA.

She investigates the capability of acoustic radiation force impulse (ARFI) and shear-wave elasticity imaging (SWEI) technologies to provide cardiac mechanical assessment for systolic and diastolic dysfunctions. Her research interests include ultrasound elastography techniques to characterize cardiac function.



Mathew Nagle received the B.S. degree in biomedical engineering from Duke University, Durham, NC, USA, in 2014 (after completing a Pratt Research Fellowship).

He is currently with the Intramural Research Program at the National Institutes of Health, Bethesda, MD, USA, investigating regenerative therapies involving pulsed focused ultrasound and stem cell homing.



Yang Jiang was born in China, in 1989. He received the B.S. degree from Zhejiang University, Hangzhou, China, in 2012, and the M.S. degree from Duke University, Durham, NC, USA, in 2014, both in biomedical engineering.

He is currently a Research Assistant working on his Ph.D. degree in bioengineering with the University of Washington, Seattle, WA, USA. His research interests include medical imaging, focusing on nonlinear imaging, and contrast-enhanced ultrasound imaging.



Gregg E. Trahey (S'83–M'85) received the B.S. and M.S. degrees in electrical engineering from the University of Michigan, Ann Arbor, MI, USA, in 1975 and 1979, respectively, and the Ph.D. degree in biomedical engineering from Duke University, Durham, NC, USA, in 1985.

He served in the Peace Corps from 1975 to 1978, and was a Project Engineer with the Emergency Care Research Institute, Plymouth Meeting, PA, USA, from 1980 to 1982. Currently, he is a Professor with the Department of Biomedical Engineering,

Duke University and holds a secondary appointment with the Department of Radiology, Duke University Medical Center. His research interests include adaptive phase correction and beamforming and acoustic radiation force imaging methods.



Patrick D. Wolf (M'89) was born in Altoona, PA, USA, in 1956. He received the B.S. degree in electrical engineering and the M.S. degree in bioengineering from Penn State University, State College, PA, USA, and the Ph.D. degree in biomedical engineering from Duke University, Durham, NC, USA.

He has been on the faculty in Biomedical Engineering at Duke University, since 1994. His research interests include instrumentation for the diagnosis and treatment of cardiac- and neural-related disease with particular emphasis on atrial

fibrillation and heart failure.